NASA TECHNICAL NOTE

NASA TN D-5403

NASA TN D-5403

EVALUATION OF AN INFRARED HEATING SIMULATION OF A MACH 4.63 FLIGHT ON AN X-15 HORIZONTAL STABILIZER

by Roger A. Fields and Andrew Vano

Flight Research Center
Edwards, Calif.

NATIONAL AERONAUTICS AND SPACE ADMINISTRATION • WASHINGTON, D. C. • SEPTEMBER 1969

1. Report No. TN D-5403	2. Government Accession No.	3. Recipient's Catalog No.
4. Title and Subtitle EVALUATION OF AN INFRARED HEATING SIMULATION OF A MACH 4.63 FLIGHT ON AN X-15 HORIZONTAL STABILIZER		5. Report Date September 1969 6. Performing Organization Code
7. Author(s) Roger A. Fields and Andrew Vano		8. Performing Organization Report No. H-560
9. Performing Organization Name and Address NASA Flight Research Center P.O. Box 273 Edwards, Calif. 93523		10. Work Unit No. 126-14-01-01-24 11. Contract or Grant No. 13. Type of Report and Period Covered Technical Note
12. Sponsoring Agency Name and Address National Aeronautics and Space Administration Washington, D. C. 20546		14. Sponsoring Agency Code

15. Supplementary Notes

16. Abstract

Temperatures recorded on the X-15 horizontal stabilizer during a Mach 4.63 flight were simulated in the laboratory. A liquid-nitrogen evaporative cooler was used to cool the structure to a prelaunch condition; the heating was provided by an infrared heating system with closed-loop control. The simulated flight produced temperatures from approximately -50° F (228° K) to 750° F (672° K). The simulation was evaluated by comparing flight-measured temperatures with those measured during the simulation.

17. Key Words Suggested by Author(s)	18. Distribution Statement
Flight heating simulation	Unclassified - Unlimited

19. Security Classif. (of this report)	20. Security Classif. (of this page)	21. No. of Pages	22. Price*
Unclassified	Unclassified	33	$3.00

*For sale by the Clearinghouse for Federal Scientific and Technical Information, Springfield, Virginia 22151.

EVALUATION OF AN INFRARED HEATING SIMULATION OF A MACH 4.63 FLIGHT ON AN X-15 HORIZONTAL STABILIZER

By Roger A. Fields and Andrew Vano
Flight Research Center

SUMMARY

Temperatures recorded on the X-15 horizontal stabilizer during a Mach 4.63 flight were simulated in the laboratory. The simulated flight involved temperatures from approximately -50° F (228° K) to 750° F (672° K). A liquid-nitrogen evaporative cooler was used to cool the structure to a prelaunch condition; the heating was provided by an infrared heating system with closed-loop control. The heater was divided into areas called zones, with feedback from a control thermocouple in each zone.

The simulation was evaluated by comparing simulation and flight temperature data. The thermocouples were grouped according to function or location on the horizontal-tail structure as follows: control, skin, web, and beam cap. The maximum average absolute temperature deviations over the complete simulated flight profile were 11 F° (6 K°) for the control thermocouples, 39 F° (22 K°) for the skin thermocouples, 30 F° (17 K°) for the web thermocouples, and 48 F° (27 K°) for the beam-cap thermocouples.

It was found that accurate temperature simulation requires liberal and judicious use of shields between control zones and at major heat-sink boundaries, minimum size of heating control zones in which a mean zone temperature is programed for control, and careful heater design.

INTRODUCTION

The loads carried by the structure of a high-speed vehicle can be classified as (1) loads caused by aerodynamic forces and (2) loads caused by thermal stress in the structure itself (ref. 1). When strain gages are used to measure these loads, some method must be utilized to establish the response of the strain gage to its thermo-structural environment.

One method of determining the thermostructural load effect of gage response to the flight environment is to observe the strain-gage output while duplicating the flight structure temperature distribution without aerodynamic loads. These responses may then be subtracted from the flight measurements to obtain aerodynamic flight load measurements.

This report evaluates a method of simulating the structure temperature distribution resulting from aerodynamic heating. Only thermocouple data were used; no attempt

was made to establish strain-gage responses. The method used infrared heating lamps with appropriate control equipment to match flight-measured temperature time histories on an X-15 horizontal stabilizer. The temperature range was approximately -50° F (228° K) to 750° F (672° K). The evaluation is based on a comparison of flight and laboratory test temperatures at selected points on the structure.

The units used for physical quantities in this report are given both in U. S. Customary Units and the International System of Units (SI). Factors relating the two systems are presented in reference 2; those used in this paper are presented in appendix A.

TEST ARTICLE

Description

The X-15 airplane, a high-speed, high-altitude research vehicle, was used by the NASA Flight Research Center to investigate the many aspects of hypersonic flight. The aircraft specifications are presented in the tables of reference 3.

The X-15 horizontal stabilizer served as a pitch and roll control and is located as shown in figure 1. The stabilizer is of conventional semimonocoque construction

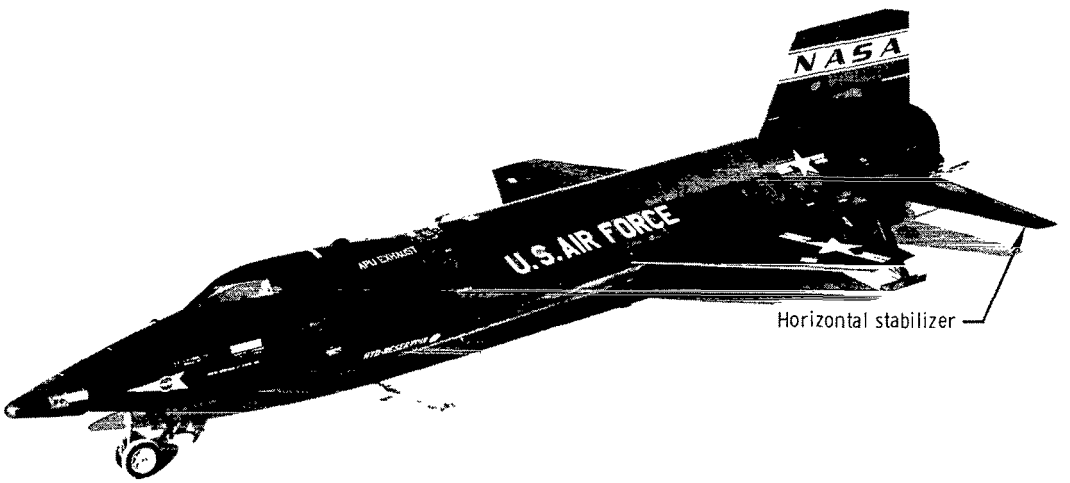

E-7910

Figure 1.– X-15 airplane.

(fig. 2). Although Inconel-X is the primary material, the aft ribs and trailing-edge beam are a titanium alloy, and the leading-edge beam is stainless steel. The total exposed surface area is 51.7 square feet (4.80 square meters). Additional structural details are presented in appendix B.

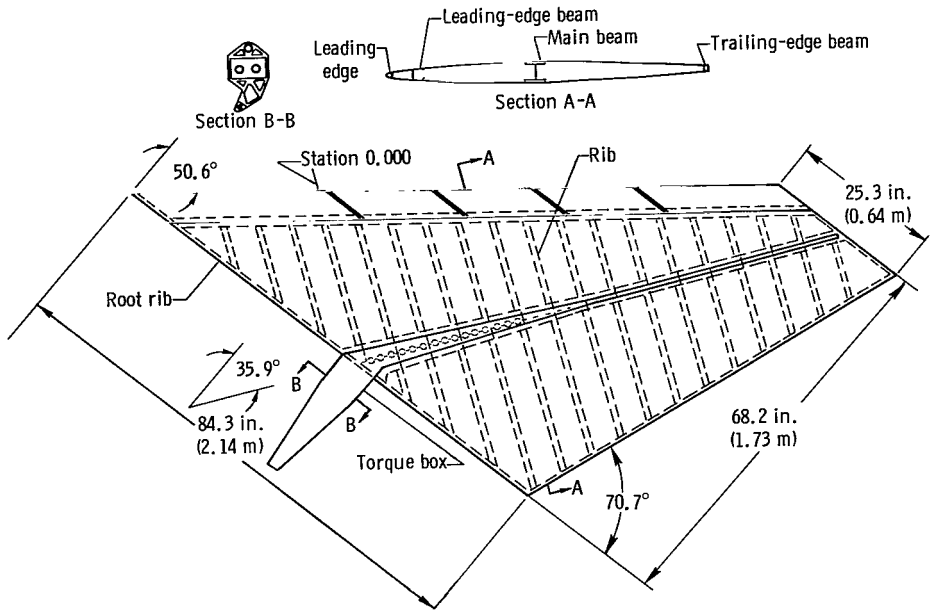

Figure 2.– X-15 horizontal-stabilizer structure.

Instrumentation

The horizontal stabilizer is instrumented internally with 121 thermocouples, and 11 thermocouples are located on the outer surface of the torque box, as shown in figure 3. Identification numbers are given in the figure only for the thermocouples specifically discussed in this report. Thirty-gage (American Wire Gauge) chromel-alumel wire was used for all thermocouples. The instrumentation installation on the aft portion

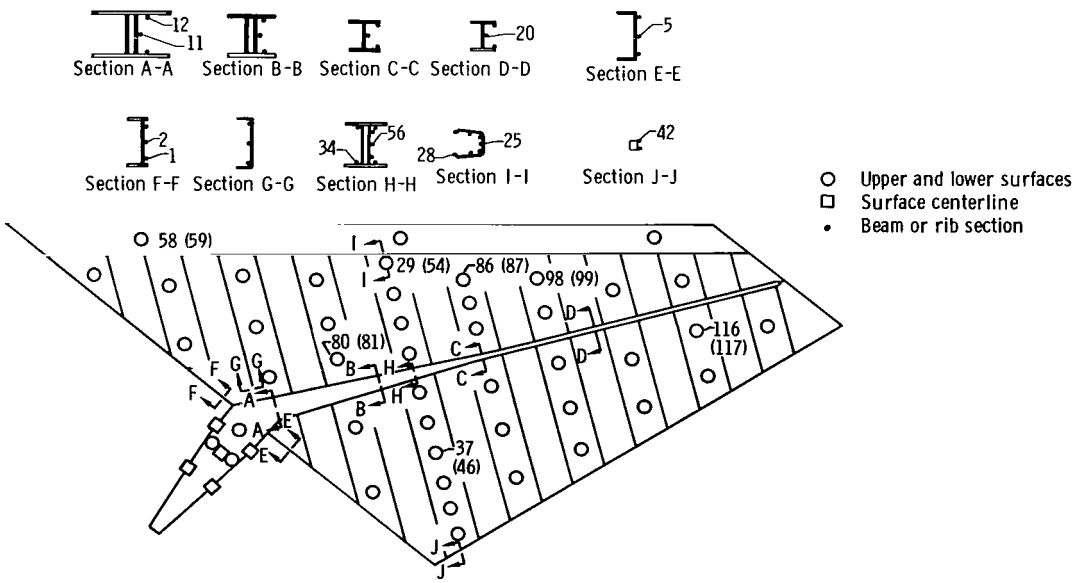

Figure 3.– Thermocouple locations on X-15 horizontal stabilizer. Sections drawn double-size; number in parentheses denotes thermocouple number on lower surface.

of the stabilizer is shown in the photograph of figure 4. Strain gages were installed adjacent to the thermocouples on beams and ribs and at all thermocouples on the skin at section A-A of figure 2. Although strain-gage data are not included in this report, the gages were operated during simulation tests since they produce a small amount of local heating.

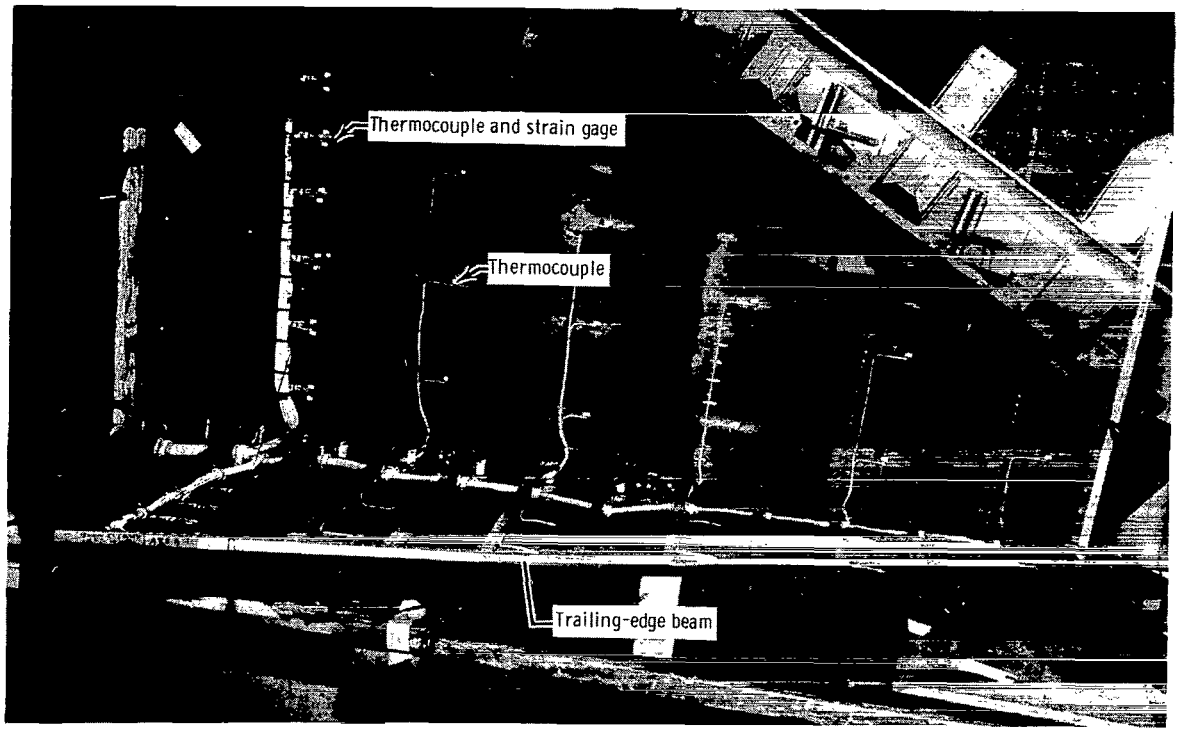

E-16076

Figure 4.– Instrumentation installation on X-15 horizontal stabilizer. (Aft panel skin removed.)

FLIGHT DESCRIPTION

The instrumented horizontal stabilizer was flown on the number 3 X-15 airplane during the flight from which the data presented in this report were obtained. The X-15 was launched from the B-52 carrier aircraft at an altitude of 46,700 feet (14,230 meters) and a Mach number of 0.82. Rocket-engine ignition occurred immediately after launch, and engine shutdown occurred about 90 seconds after launch. Immediately after shutdown, a horizontal-stabilizer load maneuver was initiated at a Mach number of approximately 4.5, an altitude of 81,000 feet (24,690 meters), and a dynamic pressure of 840 lb/ft^2 (402 hN/m^2). The maneuver consisted of a 90° left bank, a rapid increase in angle of attack to 11° and 3g normal acceleration, then a push-over to 0g.

Three other maneuvers during the flight were similar to the stabilizer load maneuver in that they were pullups to approximately 12° angle of attack and were performed at Mach numbers of 4.0, 3.7, and 2.5, dynamic pressures of approximately 635 lb/ft^2 (304 hN/m^2), 615 lb/ft^2 (295 hN/m^2), and 645 lb/ft^2 (309 hN/m^2), and flight times of 130 seconds, 150 seconds, and 220 seconds after launch, respectively.

The maximum Mach number, altitude, and dynamic pressure recorded during the flight were 4.63, 84,400 feet (25,730 meters), and 1399 lb/ft^2 (670 hN/m^2), respectively.

LABORATORY SIMULATION EQUIPMENT

Heating System

Infrared lamps were used to provide the radiant heat flux for the aerodynamic heating simulation. The lamps were mounted on polished stainless-steel reflectors of the same shape and contour as the stabilizer; the reflectors were then positioned 5.5 ±0.5 inches (13.97 ±1.27 centimeters) above and below the stabilizer to form the primary heater. The top reflector assembly is shown in figure 5. The quartz heating

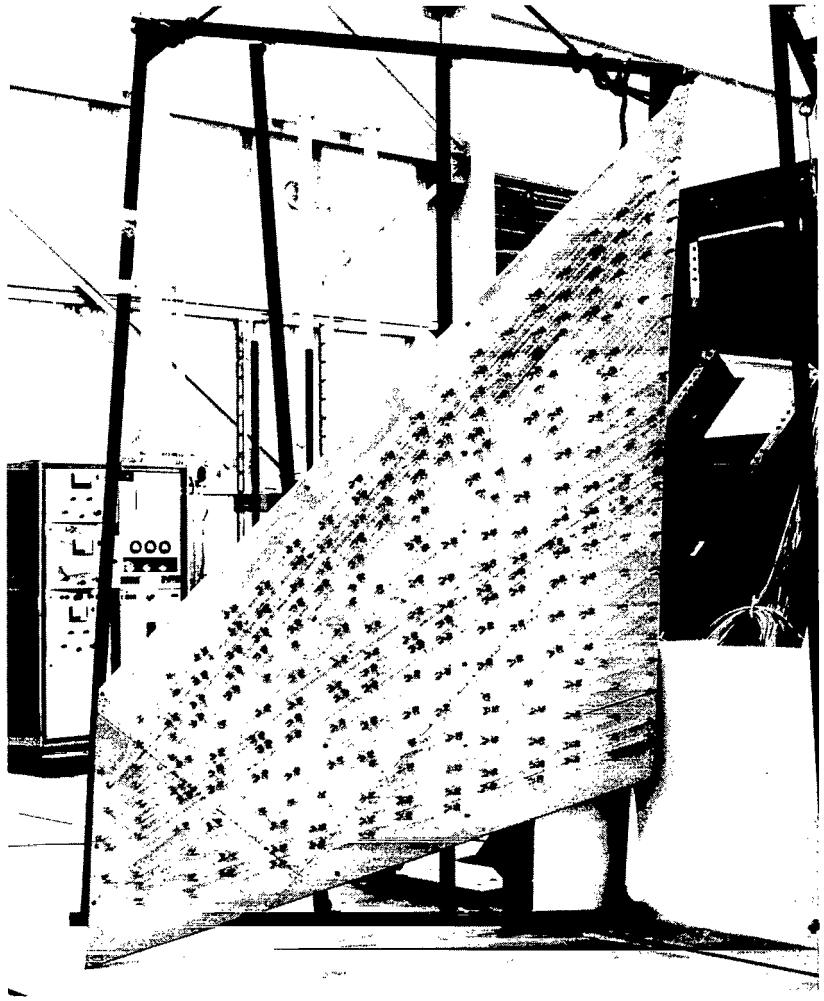

Figure 5.– Top reflector assembly for heating horizontal stabilizer.

lamps were distributed on the reflector with the highest lamp densities over the main beam, leading-edge assembly, and trailing-edge beam. No attempt was made to provide heating simulation around the stabilizer support, since this was deemed to be beyond the scope of this investigation.

The infrared heater is controlled by a closed-loop system, as illustrated by the block diagram of figure 6. A control thermocouple at a particular specimen location, chosen to be representative of the zone, generates a millivoltage which is compared with the function-generator output; this output represents the simulation temperature time history programed for the control thermocouple location. If there is a difference (error) between these two signals, the controller commands the ignitron power regulator to supply more or less power to the heater, maintaining the error near zero.

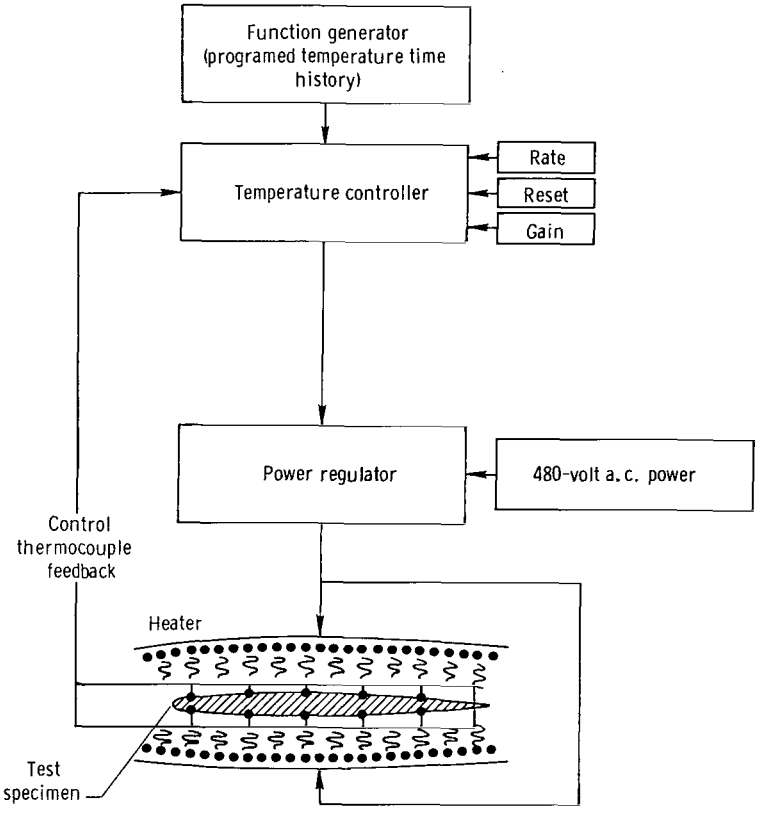

Figure 6.– Block diagram of laboratory heating system.

Typical power controller racks are shown in figure 7. Each rack contains two function generators which can program any of the six temperature controllers in the same rack. The regulator voltage for each channel and a local control board are also

E-14609

Figure 7.– Laboratory heating system power controller rack.

displayed. The test is conducted from the central control console shown in figure 8. A selected number of temperatures are monitored on the strip-chart recorders and bar-graph display during the test.

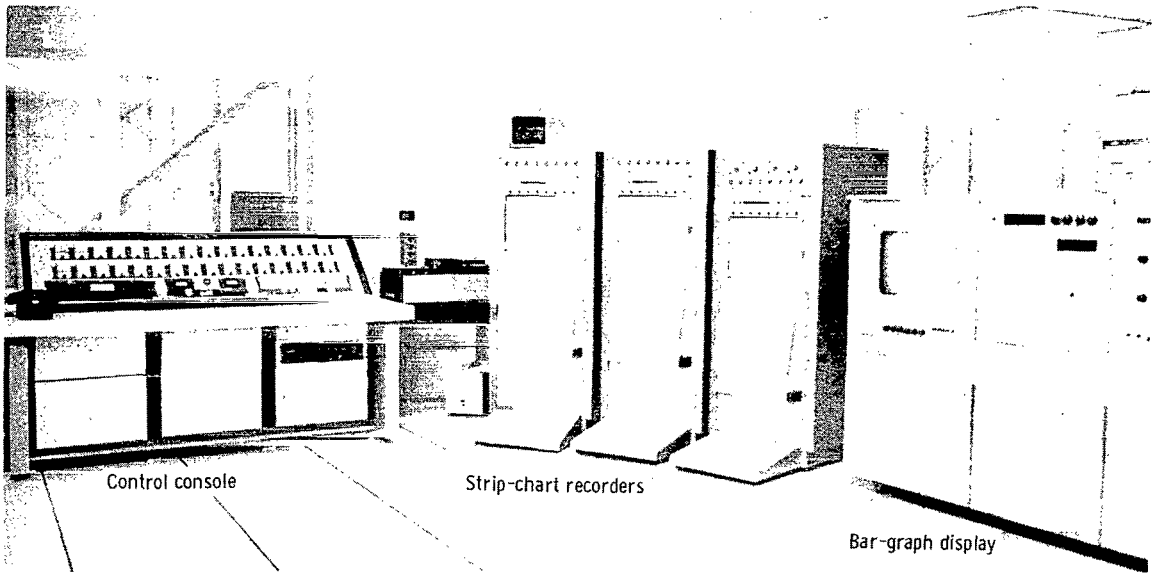

Figure 8.– Laboratory test control room.

Additional control features of the heating system that improve the temperature control are rate, reset, and gain. The rate control modifies the command signal in a way that prevents temperature overshoot caused by the thermal capacity of the heating lamps. The reset control eliminates the temperature difference between command and test specimen caused by thermal losses. The gain control adjusts the width of the proportional control band. The setting for any one of these controls depends on the setting of the others and must be experimentally established prior to the data run for minimum control error.

The temperature controller specifications are as follows:

Null measuring accuracy	±0.25 percent of full scale or 15 microvolts, whichever is greater
Repeatability	0.1 percent
Response time	20 milliseconds
Proportional-band range	0.3 percent to 30 percent for a 20-microvolt range

The specifications for the function generator are as follows:

Time-base accuracy	1.0 percent of elapsed time
Dead band	0.01 percent of full scale
Repeatability	0.05 percent of full scale
Potentiometer linearity	0.2 percent

The accuracy with which the flight temperature time histories were programed for the temperature controller was evaluated by comparing the output of the function generators with the flight data. This comparison established the programing to be within ±5 F° (±3 K°) of the flight-measured temperatures.

X-15 launch was chosen to be zero heating test time. It was found that errors in synchronizing the function generators to this time caused temperature errors of ±5 F° to ±15 F° (±3 K° to ±8 K°).

Cooling System

The simulation at a particular data event must include all significant environmental conditions beginning from some data reference. For loads measurements in which strain gages are used, the simulation must be started at the last available zero-load condition; for the X-15, this was just prior to B-52 takeoff. Thus, the horizontal-stabilizer simulation had to start at ambient conditions, cool down and cold soak to the launch condition, and then proceed to the X-15 flight heating profile.

A cooling system was constructed to provide the cool-down and cold-soak portion of the simulation. During a particular test, the cooler mixes ambient air with liquid nitrogen (LN_2), which evaporates and extracts the heat of vaporization from the ambient air, cooling it to the desired temperature. This air is then directed to the test specimen by a system of ducts.

The construction of the cooler is illustrated in figure 9; the side plate is removed

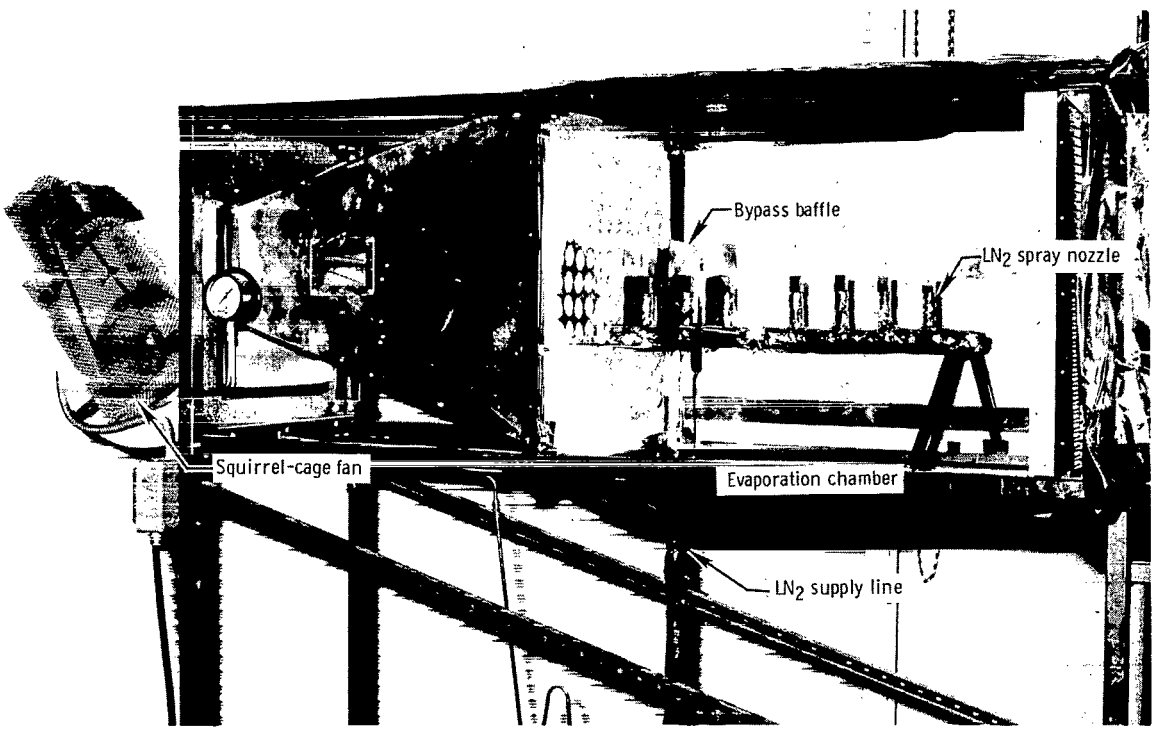

Figure 9.– Liquid-nitrogen evaporative cooler for stabilizer tests. (Side plate removed.) E-19434

to expose the interior. A squirrel-cage fan drives ambient air through an expansion nozzle into an evaporation chamber. Bypass baffles force the flow in the chamber near the walls where it mixes with LN_2 droplets sprayed from the LN_2 nozzles. The LN_2 was supplied by a portable 150-gallon (0.568-meter^3) cryogenic tank; the fluid was transferred by pressurizing the tank with a controlled LN_2 boiloff.

Temperature was controlled for a given airflow by manually regulating LN_2 line pressure such that a particular downstream duct temperature followed a predetermined profile.

DATA-RECORDING EQUIPMENT

X-15 Pulse Code Modulation System

Flight temperatures were measured by an onboard pulse code modulation (PCM) encoder; the encoded measurements were transmitted to a ground telemetry station during the flight, decommutated, and recorded on tape. The data were then reduced to temperatures by using a digital computer programed to convert system counts to degrees Fahrenheit on the basis of the chromel-alumel thermocouple table in reference 4. The accuracy of the system has been demonstrated to be better than ±0.3 percent of full scale, or ±7 F° (±4 K°) at 1500° F (1090° K) and ±10 F° (±6 K°) at -160° F (167° K).

Loads Calibration Laboratory Data-Acquisition System

The Loads Calibration Laboratory data-acquisition system consists of portable acquisition units located near the sensors and a central control system. Each portable unit provides signal conditioning, multiplexing, and 12-bit analog-to-digital conversion. The digital signal is relayed to the central control system and a high-speed digital computer shown in figure 10. The computer provides all necessary control for the data acquisition and formats the incoming digital data from the acquisition units for recording on a 9-track magnetic tape. Voltages from up to 800 transducers (400 thermocouples, 320 strain gages, and 80 potentiometers) can be recorded in ranges varying from ±5.0 millivolts full-scale with a resolution of 2.5 microvolts to ±4.0 volts with a resolution of 2.0 millivolts. The transducer signals are commutated at a nominal sampling rate of 10 samples per second per channel. The data-acquisition system can record the input voltages to an accuracy of 0.5 percent of range maximum and 0.2 percent of range typical (±1.6 F° (±0.89 K°) at 700° F (645° K) and ±2.0 F° (±1.11 K°) at -50° F (228° K) on 20-millivolt range). The largest contribution to temperature-measurement errors is made by the thermocouple itself. However, since the same thermocouples are used in flight and ground simulation, this error in the simulation tends to cancel. The thermocouples are considered to be accurate to the larger of ±5 F° (±3 K°) or ±0.75 percent of the temperature.

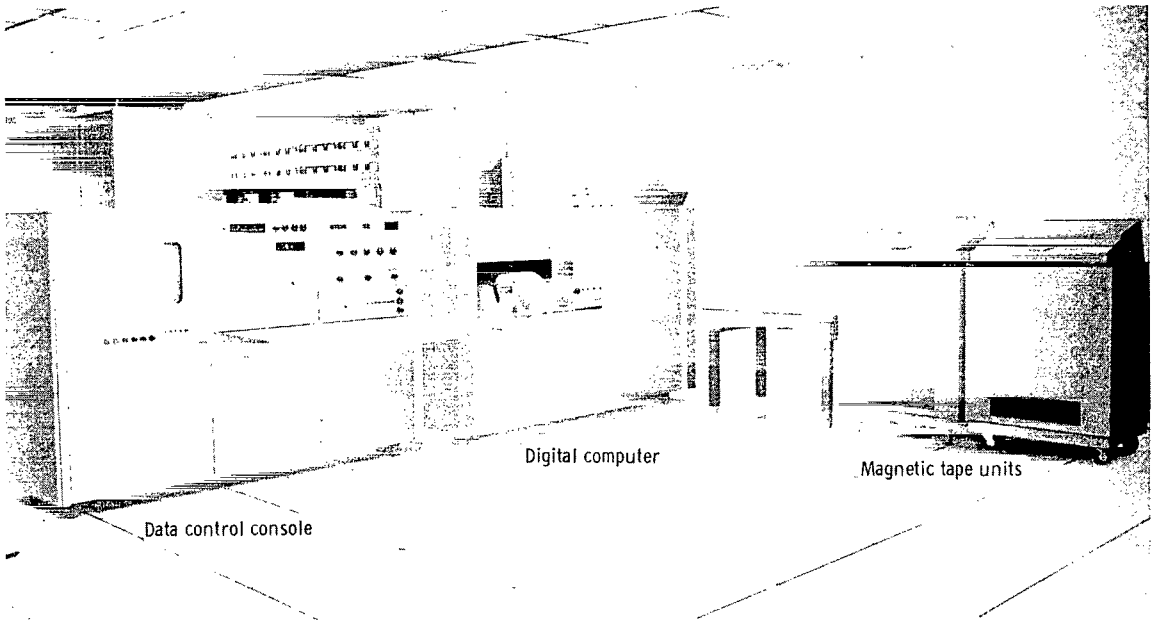

Figure 10.– Laboratory data-acquisition system central control.

DEVELOPMENT OF HEATER

Heating-Reflector Configuration

The initial distribution of the lamps into zones (areas to be controlled by one thermocouple) and within each zone is shown in figure 11; all the quartz lamps in any

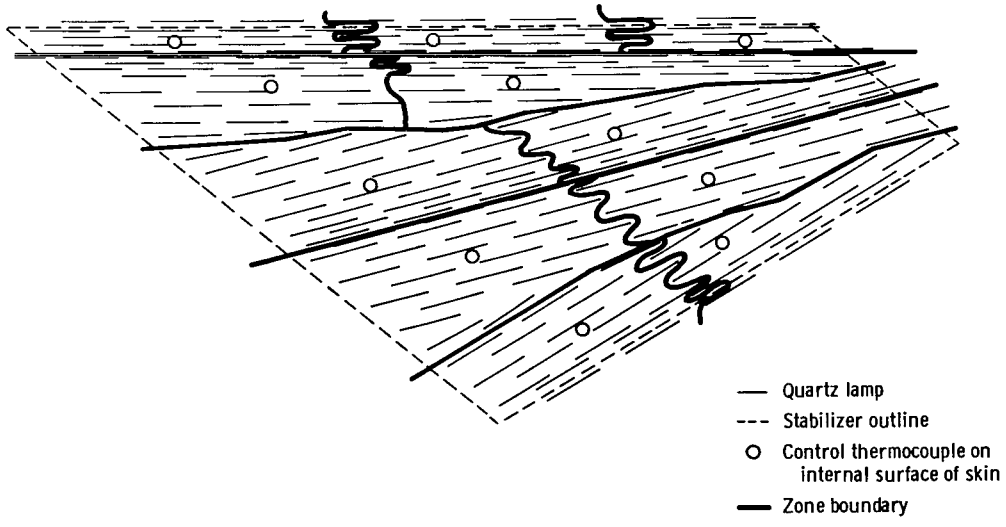

Figure 11.– Initial lamp zoning for X-15 horizontal-stabilizer heating simulation.

one zone are wired in parallel and controlled by the same regulator and therefore have the same voltage. The distribution of lamps within each zone helped provide the proper distribution of heat flux over the stabilizer surface. This configuration consisted of 222 12-inch 1000-watt lamps per reflector. The size of the control zones ranged from approximately 1.0 square foot to 3.9 square feet (0.10 square meter to 0.36 square meter), and the number of lamps per zone ranged from 11 to 26.

The preliminary heating-test results indicated that more lamps were necessary to heat the leading-edge structure. In addition, the power required to heat the leading-edge zones overheated the adjacent zones at the control-thermocouple locations, causing a lack of adequate control in these adjacent areas. This problem, known as cross-talk,[1] was corrected by installing a leading-edge heater and an asbestos shield between the leading-edge zones and adjacent zones (fig. 12).

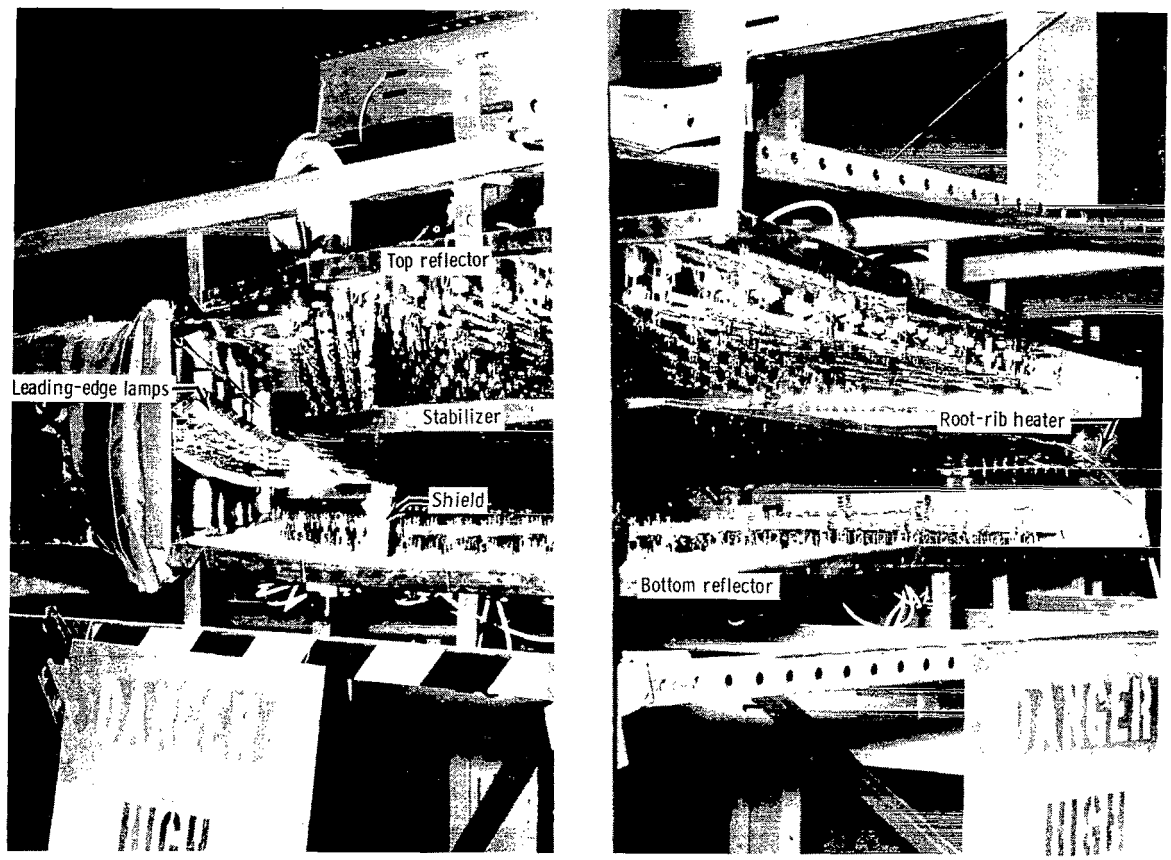

Figure 12.– Heater assembly for heating simulation on X-15 horizontal stabilizer.

[1]A condition caused by a control thermocouple being at a higher temperature than programed because of heating from outside the subject zone. This causes the power to the zone lamps to remain off until the measured temperature becomes less than that programed.

Further heating tests indicated that it would be necessary to increase the number of control zones over the stabilizer surface. Heaters were also constructed for the root rib to simulate flight heating in the gap between the stabilizer and the fuselage; the root-rib heaters were controlled by internal thermocouples on the root-rib centerline. Figure 13 shows the root-rib-heater construction. A row of lamps was installed on the root-rib reflector above the stabilizer skin surface to reduce the primary heater end effects; these lamps were wired to be part of adjacent skin control zones. Ten of the 25 lamps located parallel to the root rib are 18 inches (46 centimeters) long and are rated 1600 watts at 240 volts; the remainder are 12-inch (30-centimeter) 1000-watt lamps.

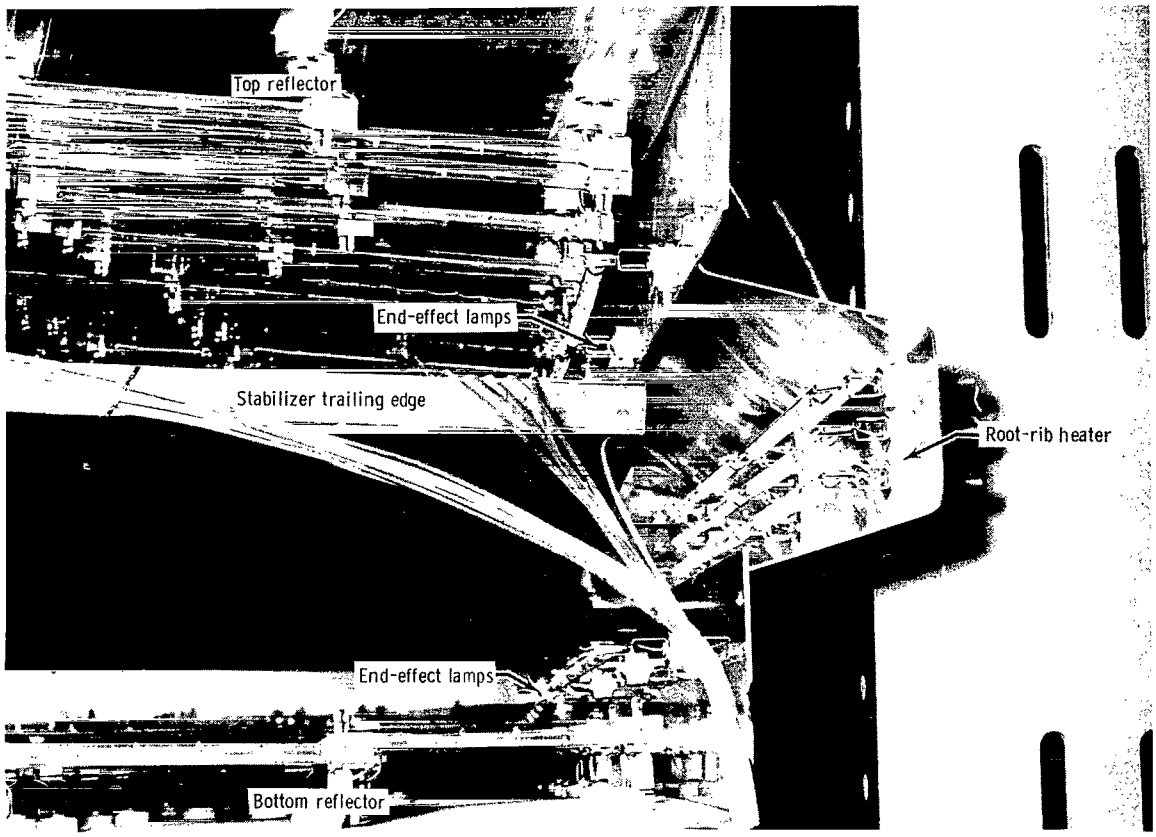

E-19436

Figure 13.– Horizontal-stabilizer root-rib heater.

The final lamp zoning configuration, composed of 36 temperature controllers and power regulators, is shown in figure 14. This configuration has 496 quartz lamps, and all were operated in the 0 to 480-volt range. The leading-edge reflector lamps, indicated by the first row of lamps in the three leading-edge zones, are controlled by the zones on the lower reflector. Additional tests indicated that it was necessary to replace the 1000-watt lamps over the stabilizer main beam with 2000-watt lamps in order to obtain increased heating in this area.

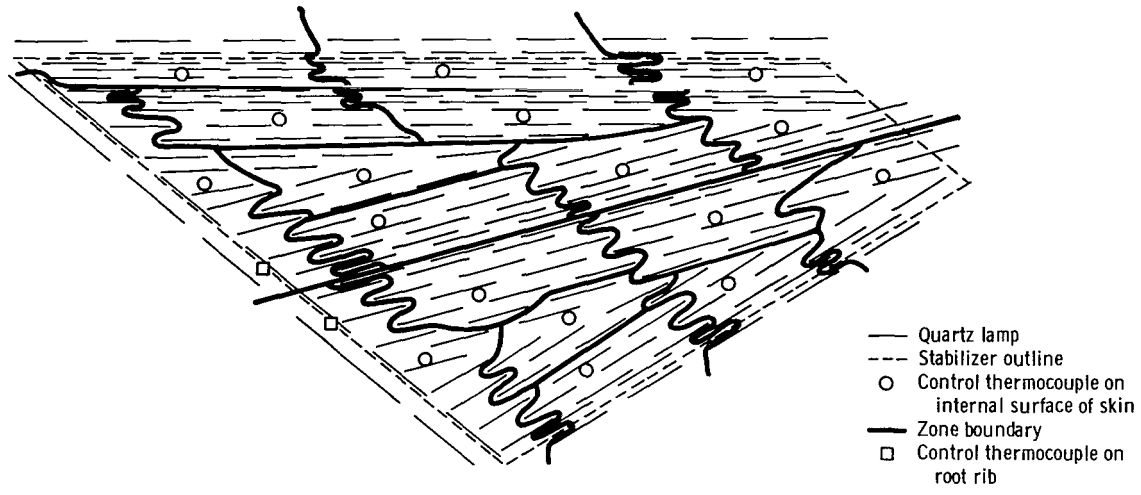

Figure 14.– Final lamp zoning for X-15 horizontal-stabilizer heating simulation.

The overall test setup in its final configuration is shown in figure 15. The power regulators are in the background; a movable data-acquisition site is shown to the right.

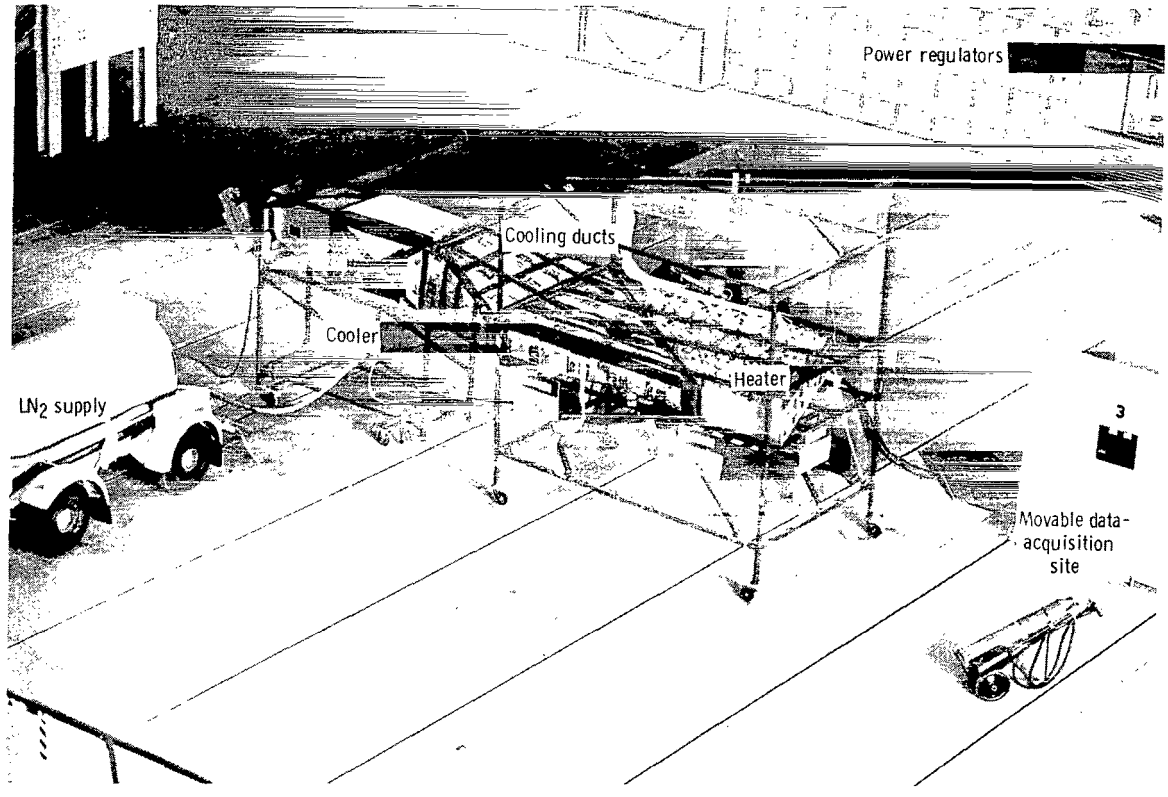

Figure 15.– Overall heating simulation test setup.

Surface Heat Flux

In-flight aerodynamic heating is a function of the difference between the recovery temperature and the surface temperature. Laboratory radiant heating is a function of the fourth powers of the lamp temperature and the surface temperature. Because of this fundamental difference in heating, it is important that lamps be distributed to accommodate this variation within a control zone, particularly in locations where there is a significant heat sink. A computer program was written during the test program to evaluate the surface flux distribution for a specified lamp configuration; the program is described in appendix C.

Lamp configuration data from the horizontal-stabilizer simulation heater at section A-A of figure 2 were entered into the lamp flux program for analysis. Figure 16 compares the net radiant flux required to maintain the flight temperature time history with that provided by the lamps as computed by the program for a time 75 seconds into the flight. The flight data points are calculated from the time-rate of change (slope) of flight temperature data and converted to a required net radiant heat flux necessary to match this slope by multiplying the specimen-absorbed heat flux by a correction factor to correct for surface reflectivity.

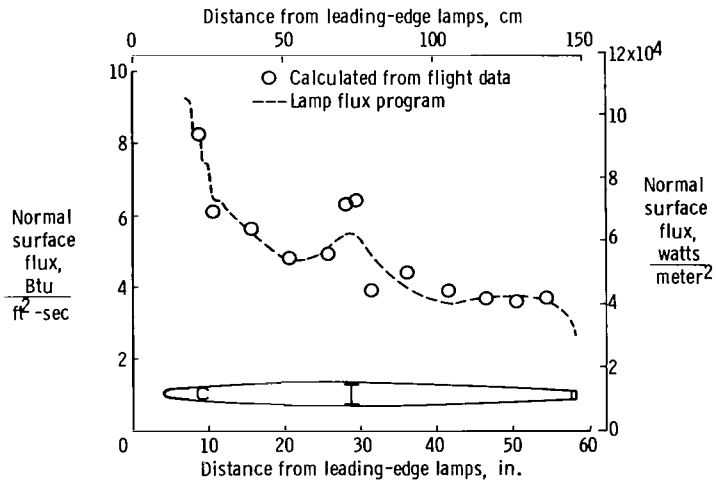

Figure 16.– Normal surface flux distribution on cross section of horizontal stabilizer.

The lamp flux program calculated the flux distribution by using a lamp power level determined by matching the total power under the calculated curve to a curve faired through the flight data points for each zone to a tolerance of ±5 percent. The leading-edge zone was not considered, since the instrumentation in this area was inadequate. A comparison of the calculated curve and the flight data indicates that the distribution is well matched except in areas where there is substructure. In these locations, the structural discontinuity is not compensated for by a corresponding flux discontinuity; this flux discontinuity could be accomplished by placing an asbestos shield between lamp zones similar to that at the leading-edge zone.

End Effects

Lamp end effects were the major source of temperature errors at the extremes of the specimen surface. The difficulty is demonstrated by curve 1 in figure 17, in which computer calculated flux distributions are plotted against distance from the specimen edge. The calculations are generated on a reflector/lamp configuration similar to that of the stabilizer. The 75-watt/inch (30-watt/centimeter) lamps were spaced 4.25 inches (10.80 centimeters) above the specimen, 1.3 inches (3.3 centimeters) below a reflector of reflectivity 0.70, and at 1-inch (2.54-centimeter) intervals over a 100-inch (254-centimeter) length. Curve 1 represents a condition in which no attempt was made to correct the end effect, and the flux dropped to 56 percent of the 8.1 Btu/ft^2-sec (919.3 hW/m^2) inboard mean value. The first attempt to improve this condition is shown as curve 2; the lamps were extended 10 inches (25.4 centimeters) beyond the surface boundary, which increased the terminal flux to 90 percent of the inboard mean.

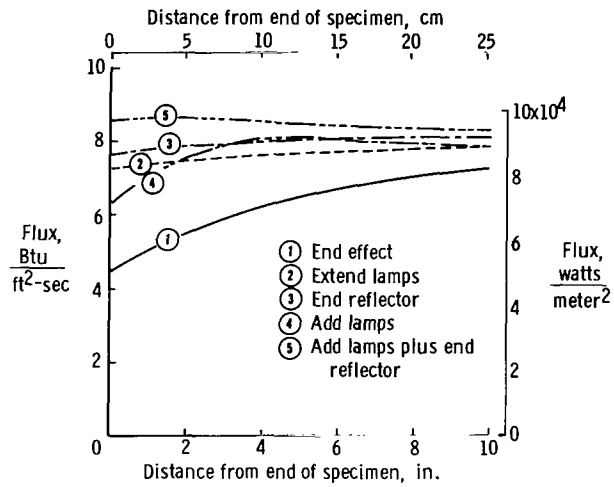

Figure 17.– Infrared heater end effects.

By locating an end reflector of 0.70 reflectivity at the surface boundary, the distribution was further improved and the flux at the terminal point was increased to 94 percent as shown in curve 3. Increasing the lamp density at the boundary by adding four lamps at 0.5 inch (1.27 centimeters), 1.5 inches (3.81 centimeters), 2.5 inches (6.35 centimeters), and 3.5 inches (8.89 centimeters) did not relieve the end effect as presented by curve 4. If a single lamp at 0.5 inch (1.27 centimeters) is added to the end-reflector configuration of curve 3, the terminal flux is greater than the inboard mean and the problem is reversed (curve 5).

The method chosen to reduce the end effect necessarily depends on the particular heating problem and the extent to which it must be reduced; the data presented indicate that an end reflector can be a useful tool in reducing this type of error.

Additional Problem Areas

Precautions must be taken during the design of the reflector to insure that the reflector shape does not change significantly enough during heating that the heating distribution is altered or the lamps and specimen contact, or both. The thermal deformations are caused by internal thermal stress, which causes reflector panel instability (buckling) and thermal expansion. The primary reflector system on the horizontal stabilizer was not designed to relieve thermal deformations, since it is relatively small and not subject to large temperature variations. A small amount of reflector buckling was observed during the test, but the deformations caused by these buckles were small enough in magnitude and mode to be considered negligible.

As first designed, the leading-edge heater consisted of a stainless steel U-shaped reflector with lamps backed by a steel Unistrut beam supported at its extremes (i.e., at the root and at the tip of the stabilizer). During heating, the thermal gradient through this heater caused the heater to deform toward the leading edge until it made contact. The design was modified by removing the Unistrut and cutting the heater into three sections, each with its own supports.

It was necessary to insure that reflector/specimen alinement was maintained between tests when the reflectors were removed for modifications.

Cooling-System Changes

Several cooling-system alterations were required during the preliminary test program. The dominant deficiency of the cooler was its inability to provide uniform temperature flow across the stabilizer span. This difficulty was caused by a nonuniform mixing of air and LN_2 in the evaporation chamber, which resulted from two factors: (1) a conical spray used to fill a rectangular section, and (2) flow reversal. The first difficulty was overcome by inserting rectangular plates along the nozzle centerline, thus causing the LN_2 to evaporate away from the nozzles. The evaporation chamber flow was improved by contouring the outside walls for a gradually increasing cross-section change.

Test Configuration and Procedure

The final heating configuration consisted of 36 control zones. The largest zone was approximately 2 square feet (0.19 square meter).

The flight-test condition of primary concern in the heating simulation was that from X-15 launch to approximately 200 seconds of free flight. The laboratory test procedure used to obtain this flight-test condition consisted of (1) cool-down and cold-soak, (2) transfer to heating mode, and (3) conduct the heating test. During the initial tests, an attempt was made to control the temperature of the ambient air that was directed over the simulation surface to a temperature profile taken from a standard atmosphere table (ref. 5) and the B-52 flight profile. During the cool-down, the heating system was programed to maintain the control thermocouple temperatures at the launch temperatures. The lamps did not operate until the temperature cooled down to the programed temperature.

This method of cool-down did not simulate aerodynamic flight conditions (such as dynamic pressure and Mach number) and so resulted in an unsatisfactory simulation. The procedure was changed to include a rapid cool-down to -50° F (228° K). As the internal structure temperatures approached launch temperatures, the air temperature was decreased to -70° F (217° K), which is the standard ambient air temperature at the launch altitude. The cooling profile is shown in figure 18 as duct air temperature data; duct 1 is farthest inboard. The cooling air was turned off as dictated by internal temperature, and the heating test was started. To prevent a sudden surge of power to the heaters, the function generators were reprogramed at the start, or zero time, to -100° F (200° K) and linearly increased to the flight temperature profile in about 5 seconds.

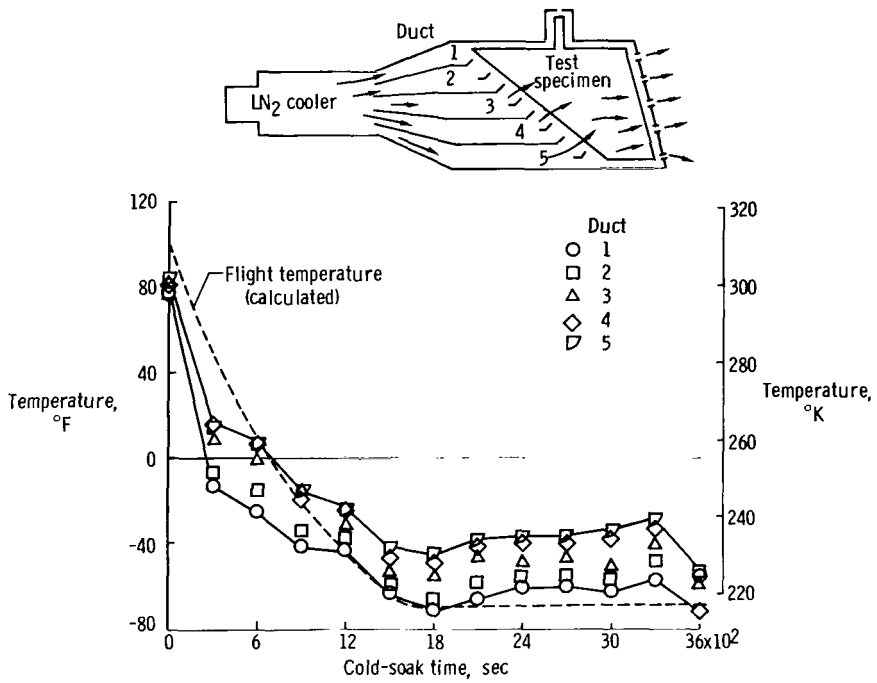

Figure 18.– Cold-soak temperature time history.

RESULTS AND DISCUSSION

Some method of processing the large volume of data obtained in this evaluation became necessary in order to compare the flight-measured temperatures with those simulated during the ground heating tests. The method chosen included the following steps: (1) The data were thinned to one sample per second; (2) flight and test simulation time histories were plotted to identical scales so that overlays could be constructed; (3) the temperature errors were measured from the overlays and tabulated for all channels at 15-second intervals, and (4) the average absolute errors were established.

The data were grouped as control, skin (other than control), beam-cap, and web thermocouples to provide a basis for comparison. Thermocouple 5, located on the

root rib as shown in figure 3, was included with the skin temperature data rather than with the control data because the lamps in that control zone did not operate. A combination of cross-talk and conduction heated the area sufficiently to maintain the temperature at the control location higher than that programed on the function generator. Typical plots of flight and simulation test temperatures for the four thermocouple groups as a function of time are shown in figures 19 to 22.

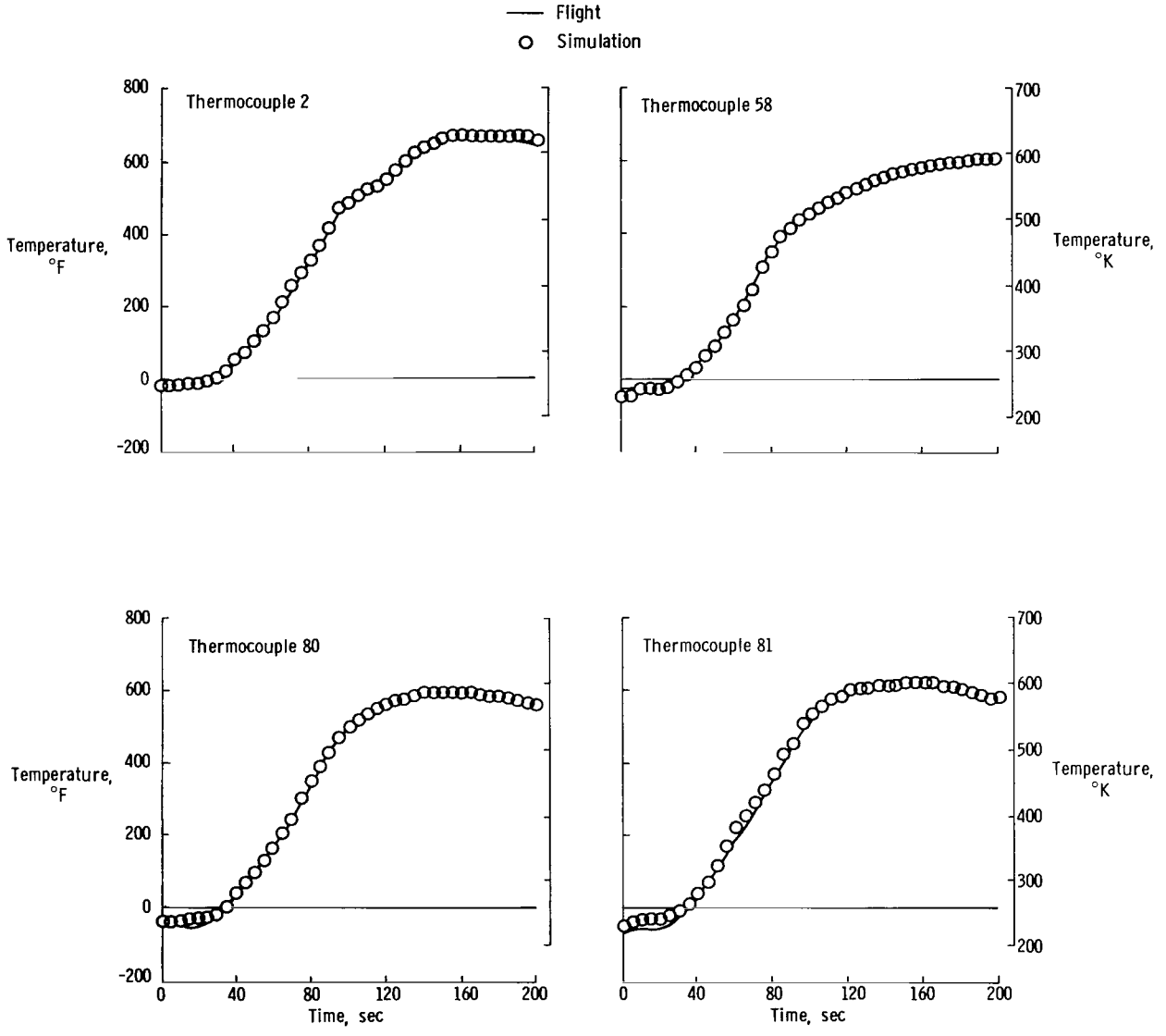

Figure 19.– Typical plots of flight and simulation test control thermocouple temperatures versus time.

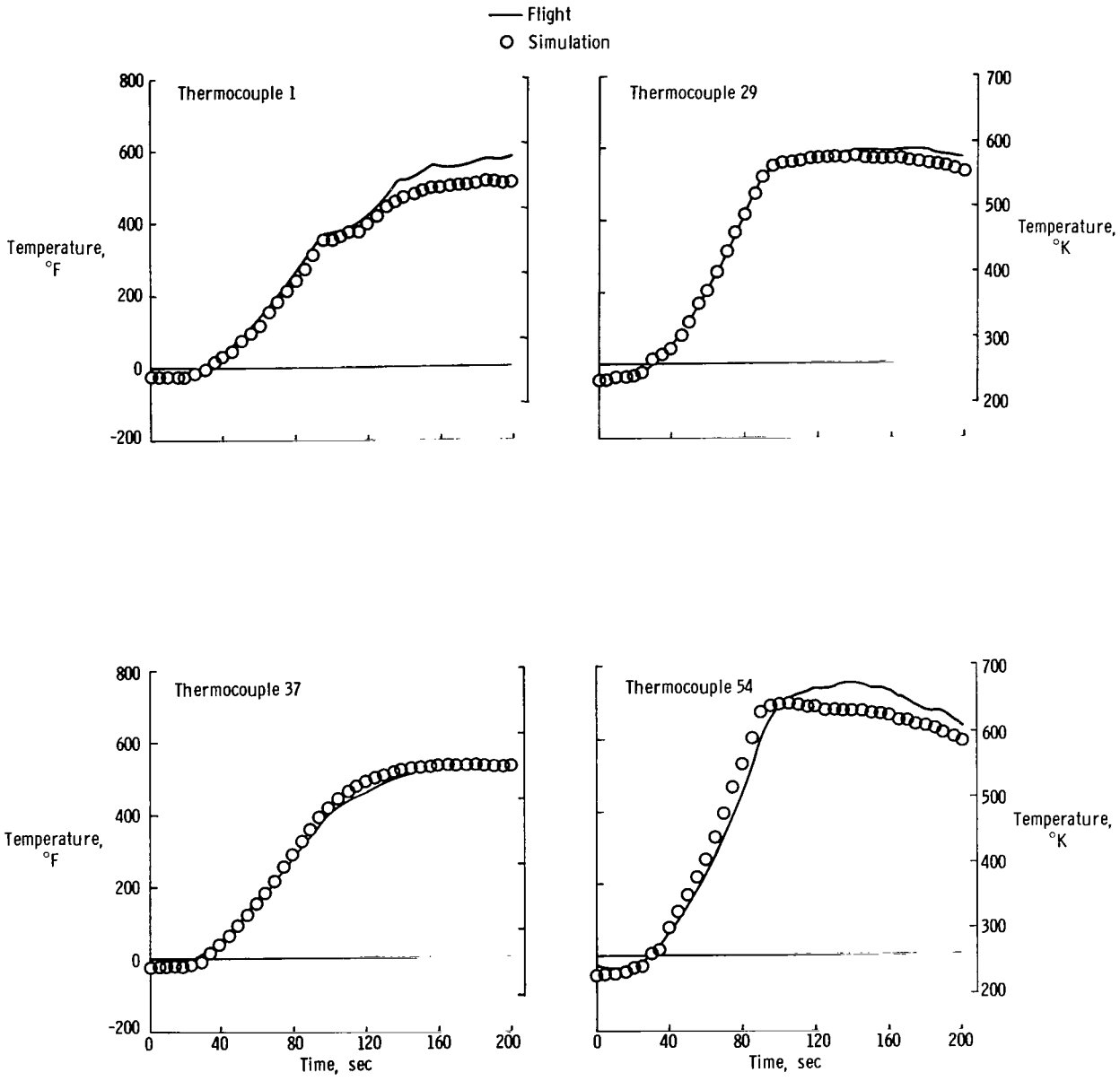

(a) Thermocouples 1, 29, 37, 54.

Figure 20.– Typical plots of flight and simulation test skin temperatures versus time.

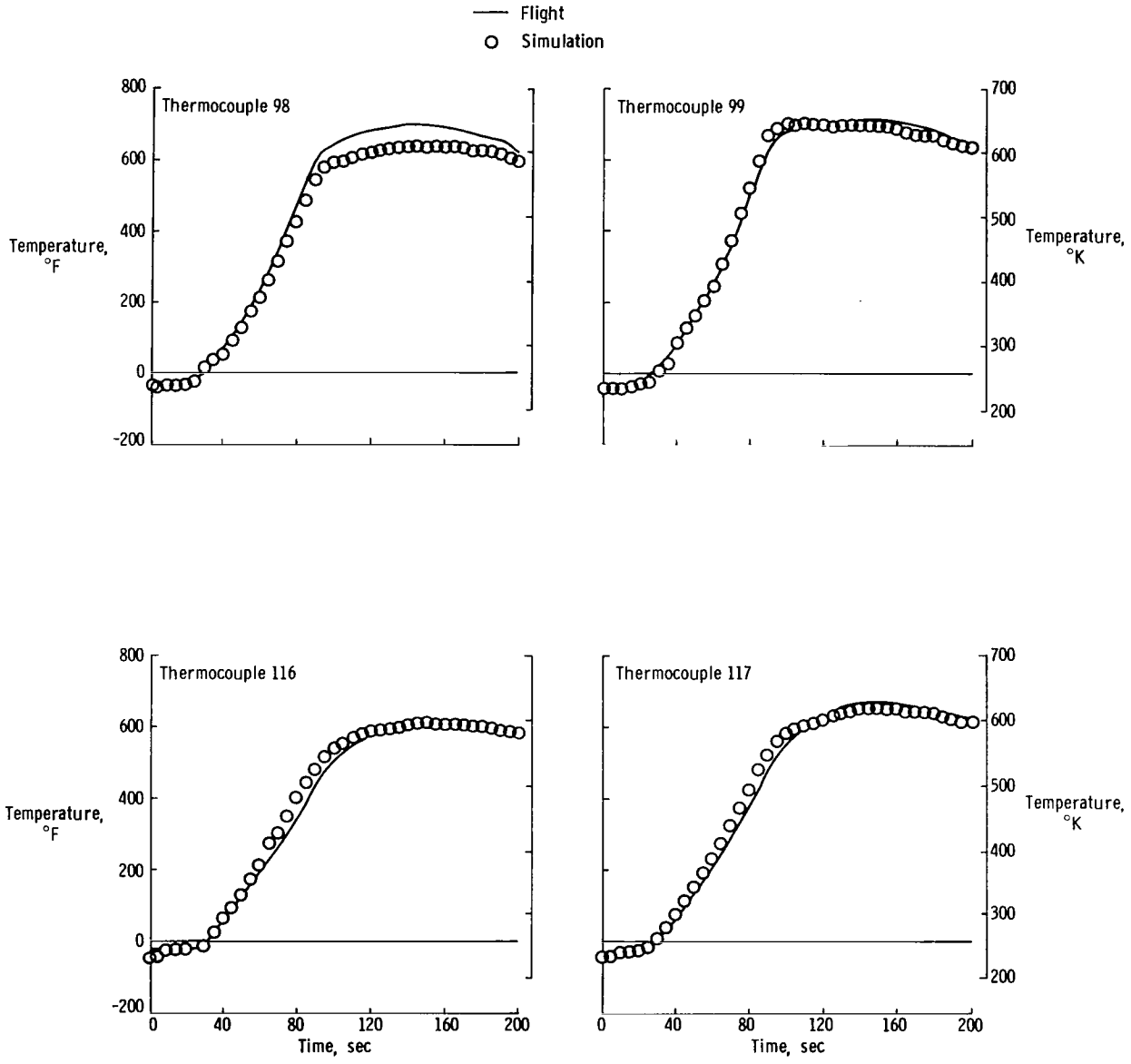

(b) Thermocouples 98, 99, 116, 117.

Figure 20.– Concluded.

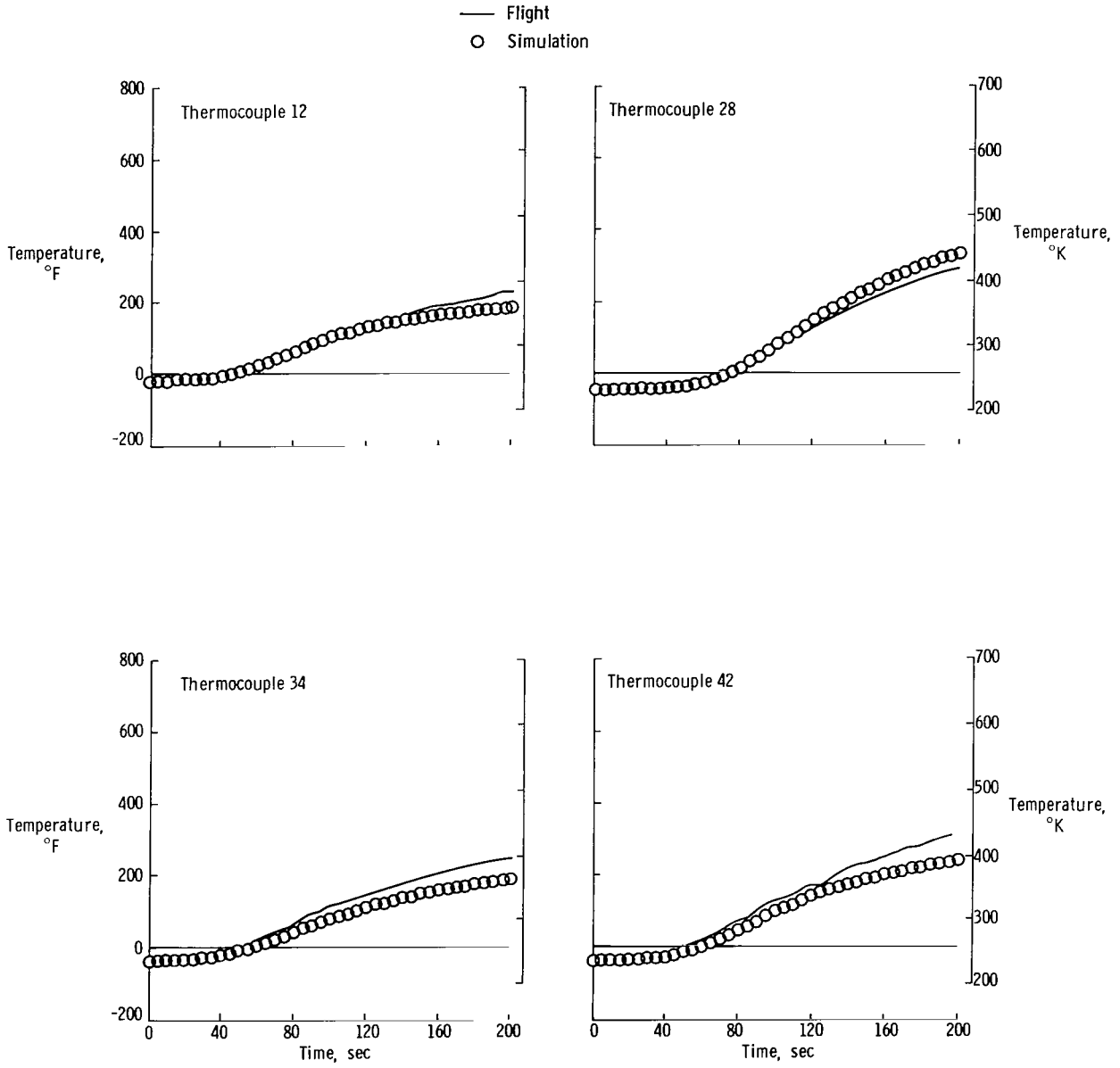

Figure 21.– Typical plots of flight and simulation test beam-cap temperatures versus time.

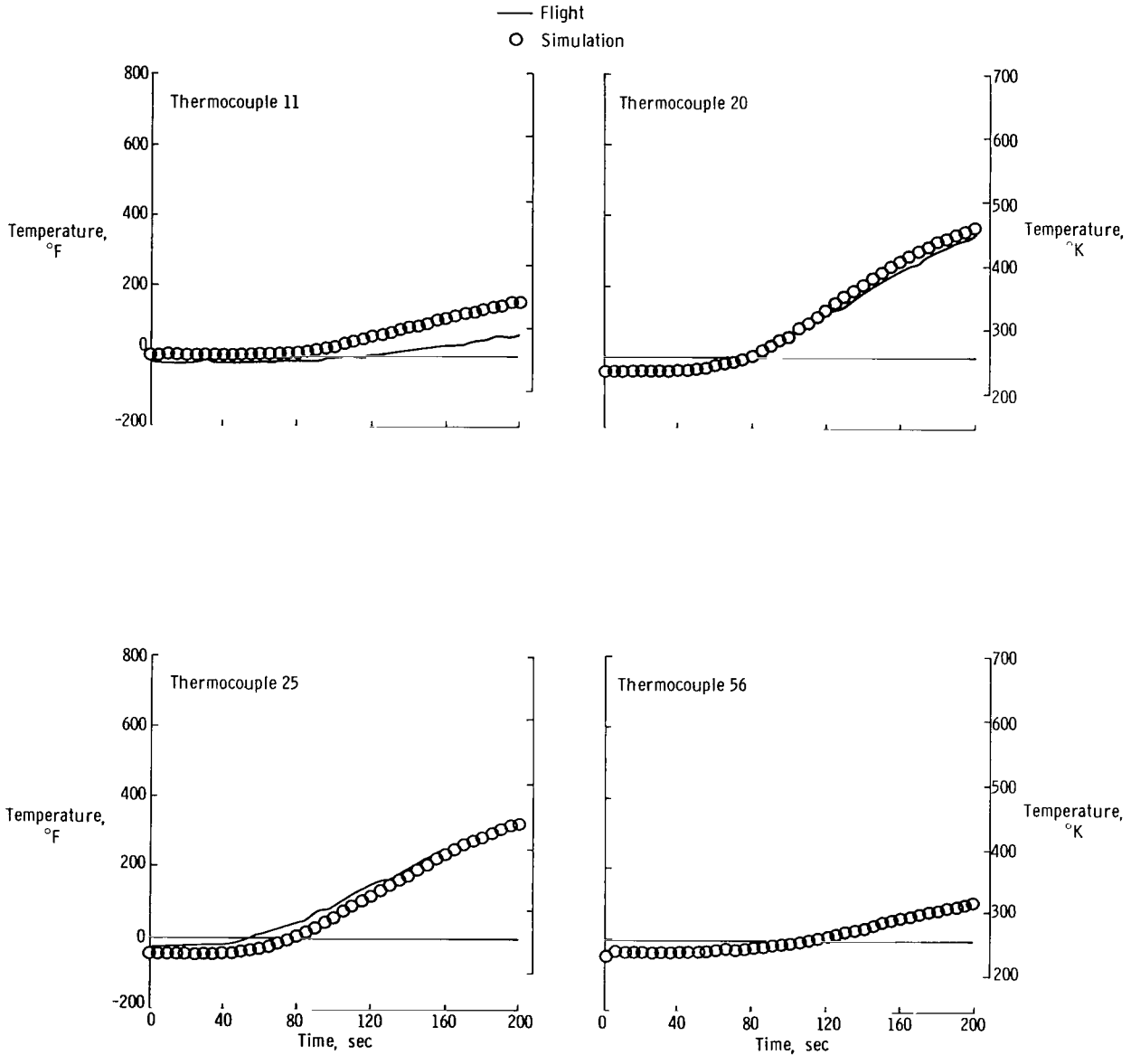

Figure 22.– Typical plots of flight and simulation test web temperatures versus time.

Figure 23 shows time histories of absolute temperature deviations for each of the four groups of thermocouples. Of all thermocouples included in each group, 25, 50, 75, and 95 percent had deviations equal to or less than the respective curves shown in the figure. The control and skin thermocouple data temperature deviations increased during the portion of the test that corresponded to the times of maximum heating rate and maximum temperature. The beam-cap (heat sink) and web (internal) thermocouple data temperature deviations increased generally throughout the test as a cumulative effect of control and skin thermocouple errors.

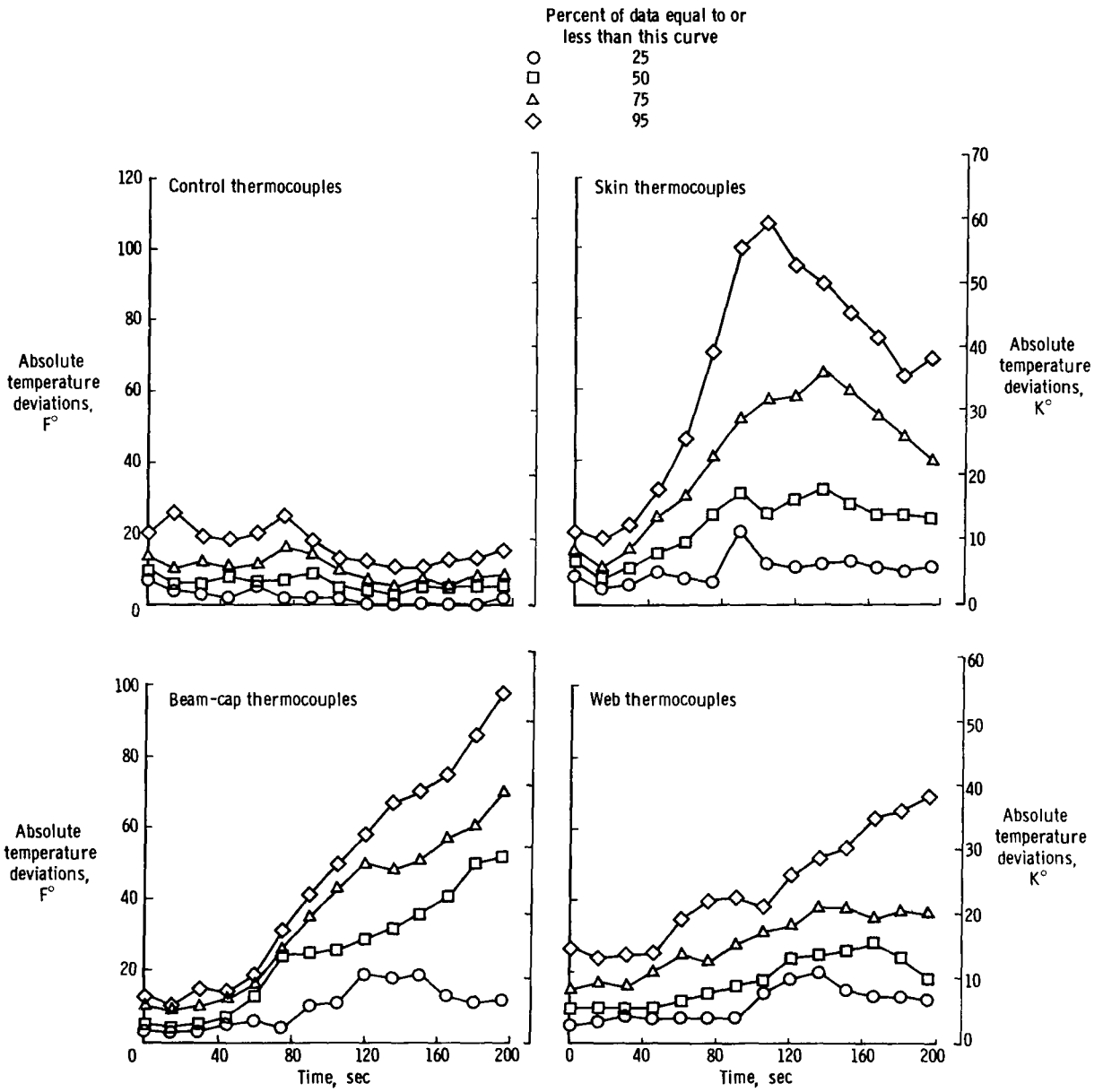

Figure 23.– Absolute deviations between flight and simulation test temperatures.

The averages of the absolute deviations between the simulation test and flight temperatures for each of the four thermocouple groups are shown plotted as a function of time in figure 24. The maximum absolute average temperature deviations for the control, skin, beam-cap, and web thermocouples are 11° F (6° K), 39° F (22° K), 48° F (27° K), and 30° F (17° K), respectively. The small temperature deviations of the control thermocouples are caused by inaccuracies in heating control equipment and errors in the program timing of the function generators.

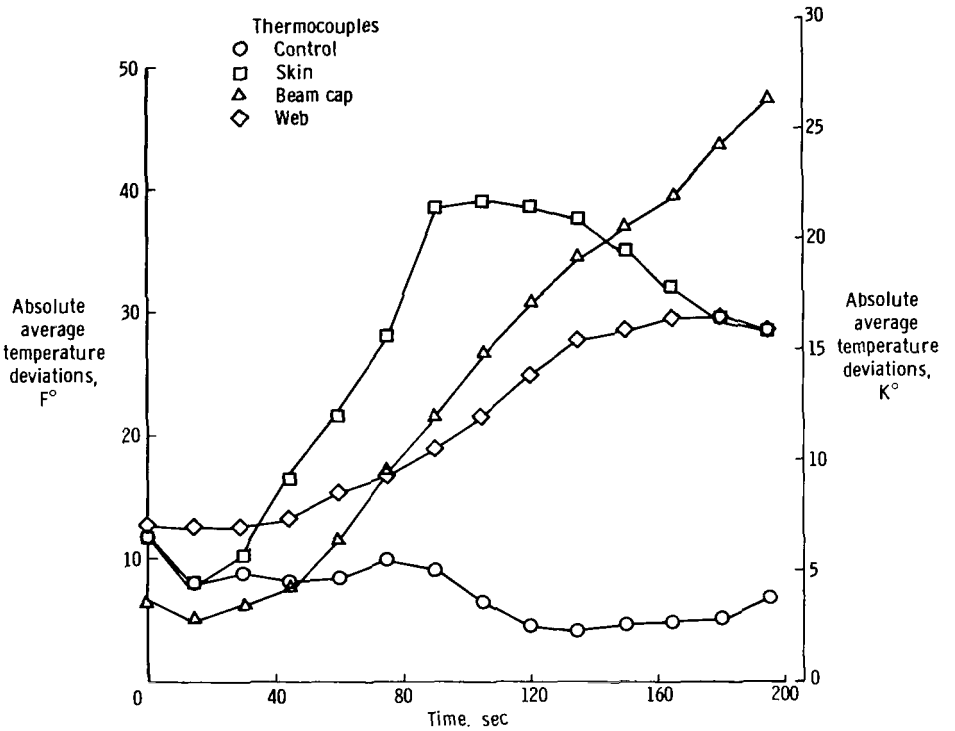

Figure 24.– Comparison of absolute average deviations between heating simulation and flight-measured temperatures for the four groups of thermocouples.

In several areas of the stabilizer, temperature deviations were large. Most of these problem areas are typified by thermocouple 54 temperatures. The simulation temperature profile for thermocouple 54 (fig. 3) as plotted in figure 25 is similar to the temperature profile programed for the heating zone that included thermocouple 54. The flight temperature profile at this location is considerably different. This situation could have been improved by programing the mean measured or calculated temperature for the entire control zone. The variation of temperatures in a control zone depends on several factors, including the control-zone size and variations in the structure and flow conditions. These temperature variations can be reduced by increasing the number of control zones and decreasing the zone area. The number of control zones will be limited by the available control equipment (as in the test discussed herein), by the size of the lamps, and by the problems associated with control cross-talk. The need for shields at control-zone boundaries increases as the size of the zone decreases.

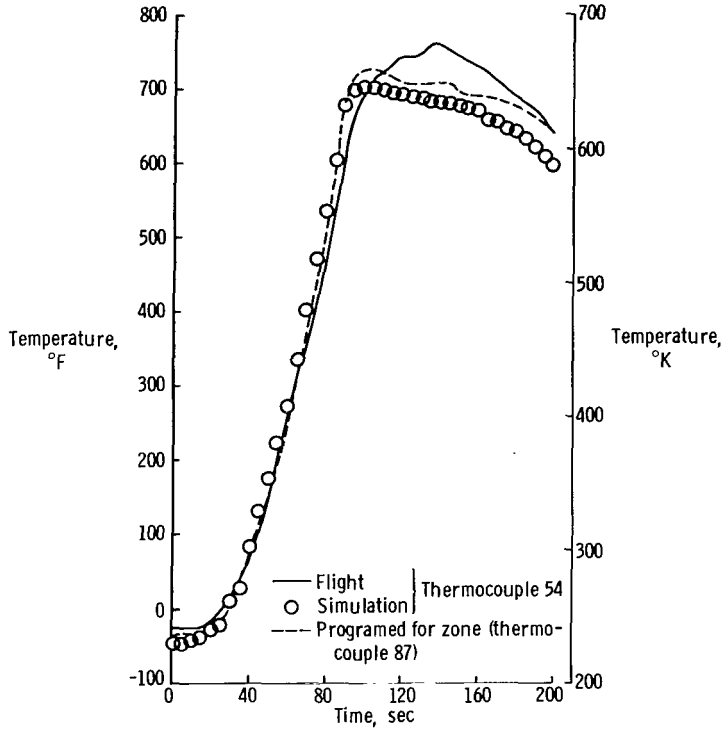

Figure 25.– Temperature variation in the heating zone that includes thermocouple 54.

Generally, the temperatures on the main-beam caps were lower during the simulation than during flight (fig. 21). However, the web temperatures at these same locations were either higher or would be higher if the cap temperatures were correct (fig. 22). The discrepancy is attributed to the fact that the thin web is heated primarily by internal radiation rather than conduction. The skin immediately adjacent to the beam cap is overheated since it receives essentially the same flux as the cap; it therefore reradiates more to the web during the simulation than during the flight, causing the web to overheat. This condition further substantiates the need for shields at the boundaries of heat sinks.

The leading-edge beam has a web three times as thick as the main beam and therefore is not as subject to heating by internal radiation. The simulation temperatures on this web were found to be close to or slightly lower than the flight temperatures.

Temperature deviations at other locations are an accumulation of errors due, in part, to the data-acquisition system, the thermocouples, the reflector design, structural discontinuities, and restricting the programing and control of the temperature profile to a single location in a zone.

CONCLUDING REMARKS AND RECOMMENDATIONS

Temperatures recorded on the X-15 horizontal stabilizer during a flight to Mach 4.63 were simulated in the laboratory. The overall simulation was considered to be

good; maximum absolute average temperature deviations were 11 F° (6 K°) for the control thermocouples, 39 F° (22 K°) for the skin thermocouples, 30 F° (17 K°) for the web thermocouples, and 48 F° (27 K°) for the beam-cap thermocouples. The temperatures at the control-thermocouple locations were close to those programed as recorded during flight. Errors at these locations were primarily inherent in the heating control equipment and the program timing of the function generators.

Temperature errors at other locations resulted from a number of factors. The overall zone temperature simulation could have been improved if the control thermocouples had been programed with a mean control zone temperature rather than the temperature time history at the location of the control thermocouples. Judicious location of shields between control zones and at significant structural discontinuities would help to eliminate cross-talk and improve local heat-flux distribution. Also, zone sizes should be kept to a minimum.

Reflector design (lamp arrangement) is an important requirement for accurate temperature control. A systematic method to derive this design is necessary. The first step must establish the design criterion; a calculated flux distribution from the flight-measured data (or other data to be simulated) can serve as this criterion. Attempts can then be made to obtain lamp distributions to match this flux distribution with appropriate discontinuities (i.e., shields) at major heat-sink boundaries. A computer program which calculates the lamp flux distributions is a valuable tool for this purpose. Heater end effects must also be considered as a part of this design.

Flight Research Center,
National Aeronautics and Space Administration,
Edwards, Calif., May 15, 1969.

APPENDIX A

CONVERSION OF U.S. CUSTOMARY UNITS TO SI UNITS

The International System of Units (SI) was adopted by the Eleventh General Conference on Weights and Measures, Paris, October 1960, in Resolution No. 12 (ref. 2). Conversion factors of the units used herein are given in the following table:

Physical quantity	U.S. Customary Unit	Conversion factor*	SI Unit
Heat flux	$Btu/(ft^2-sec)$	1.1349×10^4	W/m^2
Length	ft	0.3048	m
	in.	2.54	cm
Pressure	lb/ft^2	0.4788	hN/m^2
Temperature	$°R = °F + 460$	0.556	°K
Volume	gal	3.785×10^{-3}	m^3

*Multiply value given in U.S. Customary Unit by conversion factor to obtain equivalent values in SI Unit.

Prefixes to indicate multiple of units are:

Prefix	Multiple
centi (c)	10^{-2}
hecto (h)	10^2

APPENDIX B

HORIZONTAL-STABILIZER STRUCTURE

The leading-edge beam, main beam, trailing-edge beam, and skins of the X-15 horizontal stabilizer (fig. 2) form a two-cell torque box. The ribs are oriented perpendicular to the main-beam centerline. The skin is made from a constant-thickness, 0.050-inch (0.127-centimeter) Inconel-X sheet. The Inconel-X leading edge is designed to act as a heat sink and is constructed in five segments to relieve thermal stresses. The leading-edge beam is a U-channel made from stainless steel 0.093 inch (0.236 centimeter) thick to station 37.625 and tapered to 0.050 inch (0.127 centimeter) at the tip.

The main beam is constructed entirely of Inconel-X. The corrugated web, 0.032 inch (0.081 centimeter) thick, is double thickness from the root to station 26.875. The main-beam caps taper in width from 6.0625 inches (15.399 centimeters) at the root to 1.875 inches (4.762 centimeters) at station 37.625 and to 1.625 inches (4.128 centimeters) at station 53.750. The remainder of the outboard cap is a constant 1.625 inches (4.128 centimeters) wide. The cap thickness along the centerline of the beam tapers from 0.300 inch (0.762 centimeter) at the root to 0.096 inch (0.244 centimeter) at station 53.750 and remains constant outboard. The beam height tapers from 3.976 inches (10.099 centimeters) at the root to 1.223 inches (3.106 centimeters) at the tip. The main-beam caps extend inboard of the root rib to form the top and bottom of the structural box (torque box) that provides support for the stabilizer.

The trailing-edge beam is made from a titanium alloy. It is a solid beam 0.448 inch (1.138 centimeters) wide that tapers in height at the aft edge from 0.768 inch (1.951 centimeters) inboard to 0.178 inch (0.452 centimeter) outboard.

The ribs forward of the main beam are 0.040 inch- (0.102 centimeter-) thick Inconel-X; those aft of the main beam are 0.050 inch (0.127 centimeter) titanium alloy. The ribs are spaced 5.375 inches (13.652 centimeters) apart.

APPENDIX C

LAMP FLUX COMPUTER PROGRAM

The FORTRAN IV subset E computer program described in this appendix was written to calculate the normal surface heat flux distribution (Btu/ft^2-sec) from a parallel nonuniform radiant heater system. The program is intended to serve as a method of predicting the effectiveness of a particular infrared heating system design.

Heater Model

The heater-specimen configuration shown in the sketch below was chosen to idealize the typical test setup. N-lamps are positioned parallel to and D distance from the flat specimen surface; the lamp spacing is defined by the array Y(I), I = 1,N which is referenced to X = 0. The lamps are considered to be infinite in length (dimension perpendicular to the plane of the figure) and are backed by a reflector of reflectivity U1

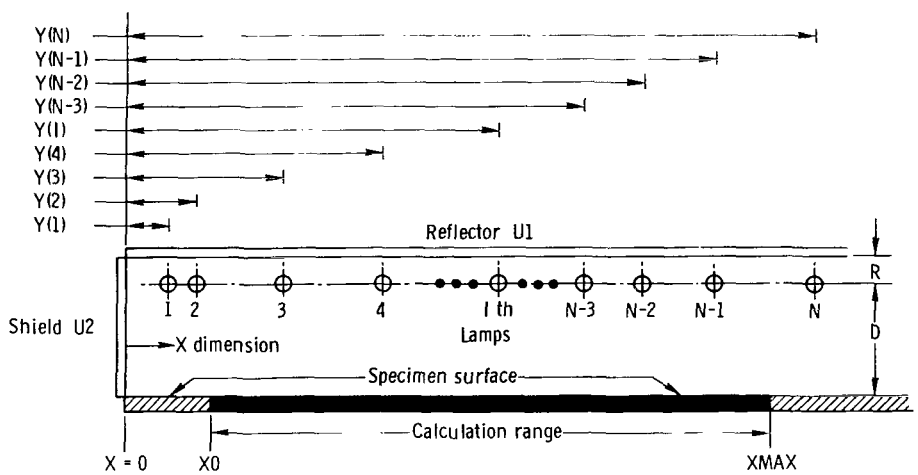

(defined as the ratio of reflected to incident radiation), which is parallel to the specimen surface and infinite in both dimensions. A shield of reflectivity U2 is positioned at the reference plane X = 0. The variables are further defined in the following table:

Variable	Definition
D	Lamp to surface dimension, real
R	Lamp to reflector U1 dimension, real
U1	Reflector reflectivity, real
U2	Shield reflectivity, real
M	Number of X calculation locations, integer, $M = \left(\frac{XMAX - X0}{XINC}\right) + 1$
N	Number of lamps, integer
X0	X value at start of calculations, real
XINC	Calculation interval, real
Y(I)	Shield to i th lamp dimension (array), real
WATT	Lamp output: watts/inch, real

APPENDIX C

The calculation range starts at X = X0 and moves to XMAX in M number of XINC increments as defined by the equation. The lamp output is defined by the parameter WATT and represents the lamp rating in watts per inch at the selected power level.

The idealization suffers from a parallel lamp-reflector-surface restriction and a uniform longitudinal lamp assumption; however, by choosing suitable geometry and reflector/shield configurations, a large spectrum of problems can be solved.

Method of Calculation

A superposition method is used to calculate the specimen surface flux. The flux at a particular X is calculated by using an inverse flux/distance-to-lamp relationship which is corrected for angle of incidence. The flux is then summed for each lamp by using the program listing below and the equation on the following page.

Program listing

```
      DIMENSION Y(500)
    1 READ(1,2)D,R,U1,U2,M,N,X0,XINC,WATT,(Y(I),I=1,N)
    2 FORMAT(2F6.2,2F5.2,2I4,2F6.2,F8.2/(12F6.1))
      IF(D-999.99)3,4,4
    3 READ(1,5)
      WRITE(3,5)
    5 FORMAT(50H
      WRITE(3,12)
   12 FORMAT(54HO CALCULATION PARAMETERS D,R,U1,U2,M,N,X0,XINC,WATT,YS)
      WRITE(3,2)D,R,U1,U2,M,N,X0,XINC,WATT,(Y(I),I=1,N)
      WRITE(3,11)
   11 FORMAT(57HO X(IN)     BTU/FT2-SEC     DIR       REF       SHD       RESH
     1D)
      REAL K0,K1,K2,K3,K4,K5
      K0=D**2
      K1=D+2*R
      K2=U1*K1
      K3=U2*D
      K4=U2*K2
      K5=K1**2
    6 DO 7 I=1,M
      X=X0+(I-1)*XINC
      SUMW=0
      SUMW1=0
      SUMW2=0
      SUMW3=0
      SUMW4=0
    8 DO 9 J=1,N
      V2=Y(J)+X
      V3=Y(J)-X
      V4=V2**2
      V5=V3**2
      W1=D/(2*3.1416*(K0+V5))
      W2=K2/(2*3.1416*(K5+V5))
      W3=K3/(2*3.1416*(K0+V4))
      W4=K4/(2*3.1416*(K5+V4))
      W=W1+W2+W3+W4
      SUMW=SUMW+W
      SUMW1=SUMW1+W1
      SUMW2=SUMW2+W2
      SUMW3=SUMW3+W3
    9 SUMW4=SUMW4+W4
      DIR=SUMW1/SUMW
      REF=SUMW2/SUMW
      SHD=SUMW3/SUMW
      RESD=SUMW4/SUMW
      BTU=0.1365*SUMW*WATT
    7 WRITE(3,10)X,BTU,DIR,REF,SHD,RESD
   10 FORMAT(F8.2,F11.3,'  ',2P4F9.2)
      GO TO 1
    4 WRITE(3,13)
   13 FORMAT('0END CALCULATIONS')
      STOP
      END
```

APPENDIX C

$$\text{FLUX}\left(\frac{\text{Btu}}{\text{ft}^2\text{-sec}}\right) = \left(\frac{0.1365}{2\pi}\right)(\text{WATT}) \sum_{J=1}^{N} \left[\frac{D}{D^2 + (Y(J) - X)^2} + \frac{U1(D + 2R)}{(D + 2R)^2 + (Y(J) - X)^2} + \frac{U2(D)}{D^2 + (Y(J) + X)^2} + \frac{U1(U2)(D + 2R)}{(D + 2R)^2 + (Y(J) + X)^2}\right]$$

The first term of the equation represents the normal surface flux due to direct radiation; the second term, that due to radiation reflected from the parallel reflector U1. The third term represents the normal surface flux caused by radiation from the vertical X = 0 reflector U2, and the last term calculates the radiation coming from both reflectors U1 and U2. The program is written to calculate flux in U. S. Customary Units; the constant (0.1365) must be changed if flux in other units is desired.

Input

To use the program a punched data deck must be generated according to the following format:

Parameter	D	R	U1	U2	M	N	X0	XINC	WATT
Columns	1-6	7-12	13-17	18-22	23-26	27-30	31-37	37-42	43-50
Decimal	4	10	15	20	INT	INT	34	40	48

Card 1: Control information

Parameter	Y(1)	Y(2)	Y(3)	Y(4)	Y(5)	Y(6)	Y(7)	Y(8)	Y(9)	Y(10)	Y(11)	Y(12)
Columns	1-6	7-12	13-18	19-24	25-30	31-36	37-42	43-48	49-54	55-60	61-66	67-72
Decimal	5	11	17	23	29	35	41	47	53	59	65	71

Lamp array cards (typical)

Parameter	Any title
Columns	2-50

Title card

Enter	999.99	0.0	0.0	0.0	1	1	0.0	0.0	0.0
Columns	1-6	7-12	13-17	18-22	23-26	27-30	31-36	37-42	43-50
Decimal	4	10	15	20	INT	INT	34	40	48

Enter	0.0
Columns	1-6
Decimal	4

Stop cards

This data deck is then used with the lamp flux object deck. As many problems (data sets) as required may be processed at one time by stacking groups of the control information, lamp array, and title cards in order. The lamp array is limited to 500 lamps per problem. The two-card stop is required to terminate the calculation.

REFERENCES

1. Wilson, Earl J.: Use of Strain Gages for Measurements of Flight Loads in a High-Temperature Environment. Preprint 68-555, Instr. Soc. Am., Oct. 28-31, 1968.

2. Mechtly, E. A.: The International System of Units. Physical Constants and Conversion Factors. NASA SP-7012, 1964.

3. Quinn, Robert D.; and Olinger, Frank V. (With appendix A by James C. Dunavant and Robert L. Stallings, Jr.): Heat-Transfer Measurements Obtained on the X-15 Airplane Including Correlations With Wind-Tunnel Results. NASA TM X-1705, 1969.

4. Shenker, Henry; Lauritzen, John I., Jr.; Corruccini, Robert J.; and Lonberger, S. T.: Reference Tables for Thermocouples. Nat. Bur. Standards Cir. 561, U.S. Dept. Commerce, 1955. (Supersedes Circular 508.)

5. International Civil Aviation Organization; and Langley Aeronautical Laboratory: Standard Atmosphere-Tables and Data for Altitudes to 65,800 Feet. NACA Rept. 1235, 1955. (Supersedes NACA TN 3182.)

NATIONAL AERONAUTICS AND SPACE ADMINISTRATION
WASHINGTON, D. C. 20546

OFFICIAL BUSINESS

FIRST CLASS MAIL

POSTAGE AND FEES PAID
NATIONAL AERONAUTICS AND
SPACE ADMINISTRATION

POSTMASTER: If Undeliverable (Section 158 Postal Manual) Do Not Return

"The aeronautical and space activities of the United States shall be conducted so as to contribute . . . to the expansion of human knowledge of phenomena in the atmosphere and space. The Administration shall provide for the widest practicable and appropriate dissemination of information concerning its activities and the results thereof."

—NATIONAL AERONAUTICS AND SPACE ACT OF 1958

NASA SCIENTIFIC AND TECHNICAL PUBLICATIONS

TECHNICAL REPORTS: Scientific and technical information considered important, complete, and a lasting contribution to existing knowledge.

TECHNICAL NOTES: Information less broad in scope but nevertheless of importance as a contribution to existing knowledge.

TECHNICAL MEMORANDUMS: Information receiving limited distribution because of preliminary data, security classification, or other reasons.

CONTRACTOR REPORTS: Scientific and technical information generated under a NASA contract or grant and considered an important contribution to existing knowledge.

TECHNICAL TRANSLATIONS: Information published in a foreign language considered to merit NASA distribution in English.

SPECIAL PUBLICATIONS: Information derived from or of value to NASA activities. Publications include conference proceedings, monographs, data compilations, handbooks, sourcebooks, and special bibliographies.

TECHNOLOGY UTILIZATION PUBLICATIONS: Information on technology used by NASA that may be of particular interest in commercial and other non-aerospace applications. Publications include Tech Briefs, Technology Utilization Reports and Notes, and Technology Surveys.

Details on the availability of these publications may be obtained from:

SCIENTIFIC AND TECHNICAL INFORMATION DIVISION

NATIONAL AERONAUTICS AND SPACE ADMINISTRATION

Washington, D.C. 20546